

Research Paper

A medicinal and edible formula YH0618 ameliorates the toxicity induced by Doxorubicin via regulating the expression of Bax/Bcl-2 and FOXO4

Jieshu You^{1,2}, Fei Gao², Hailin Tang³, Fu Peng², Lei Jia², Kun Huang⁴, Kinlong Chow², Jiaqi Zhao^{2,5}, Huanlan Liu¹, Yi Lin⁶, Jianping Chen²✉

1. Basic Medical College, Guangzhou University of Chinese Medicine, Guangzhou, Guangdong Province, China.
2. School of Chinese Medicine, The University of Hong Kong, Hong Kong, China.
3. Galactophore Department, Sun Yat-Sen University Cancer Center, Guangzhou, Guangdong Province, China.
4. School of Biological Science, The University of Hong Kong, Hong Kong, China.
5. College of pharmacy, Chengdu University of Chinese Medicine, Chengdu, Sichuan Province, China.
6. Galactophore Department, Guangdong Provincial Hospital of Chinese Medicine, Guangzhou, Guangdong Province, China.

✉ Corresponding author: Dr. Chen Jianping, School of Chinese Medicine, The University of Hong Kong, 10 Sassoon Road, Pokfulam, Hong Kong. Tel.: +852 39176479; Fax: +852 21684259; E-mail address: abchen@hku.hk

© Ivyspring International Publisher. This is an open access article distributed under the terms of the Creative Commons Attribution (CC BY-NC) license (<https://creativecommons.org/licenses/by-nc/4.0/>). See <http://ivyspring.com/terms> for full terms and conditions.

Received: 2019.01.02; Accepted: 2019.05.04; Published: 2019.06.09

Abstract

Chemotherapy is the most common and powerful cancer treatment. Although the nasty side effects seriously influence the clinical practice, no better ways can displace it. Therefore, searching for safe and effective strategies designed to ameliorate chemotherapy-induced toxicity has become an urgent issue in cancer research area. In clinical, a medicinal and edible formula YH0618 showed the effects of reducing the DOX-induced toxicity, especially improving alopecia, nail discoloration, skin hyperpigmentation and fatigue. This study was to investigate the role and mechanism of YH0618 in ameliorating DOX-induced toxicity by *in vitro* and *in vivo* experiments. YH0618 selectively attenuated DOX-induced growth inhibition and apoptosis in human normal liver L02 cells and kidney HEK-293 cells, and simultaneously potentiated the anti-cancer effect of DOX in breast cancer MCF-7 and MDA-MB-231 cells by apoptosis pathways. Western blotting results revealed that YH0618 attenuated DOX-induced apoptosis in normal liver and kidney cells through FOXO4-mediated mitochondria-dependent mechanism. Animal experiments demonstrated that, YH0618 did not interfere in DOX-induced reduction in tumor volume and significantly improved DOX-induced hair loss and the increase of alanine aminotransferase (ALT). Histological characteristics showed that YH0618 attenuated DOX-induced heart, liver and kidney damage. The study may shed light on the potential application of YH0618 as a novel medicinal food against chemotherapy-induced toxicity.

Key words: Medicine and food homology; YH0618; DOX-induced toxicity; Apoptosis; Bcl-2/Bax; FOXO4

1. Introduction

Chemotherapy, as a standard regimen, has been used for cancer treatment for more than 75 years and proved to be useful in most cancer treatments in combination with surgery [1]. However, the effectiveness of chemotherapy is often limited by its severe toxicity and side effects because chemotherapy damages other normal tissues simultaneously when it kills cancer cells. As chemotherapy remains primary position in cancer treatment and no better regimen can replace it, therefore, searching for safe and effective ways for ameliorating chemotherapy-

induced toxicity has become an urgent issue in cancer research area.

Recently, multiple options for reducing chemotherapy-induced toxicity (CIT) have been investigated, but there are no acknowledged and standard treatments yet. Chemical drugs are the mainstream for relieving CIT, but they have an opportunity to induce other side effects and the effectiveness is uncertain [2-4]. Chinese medicine-based therapy for improving the efficacy and reducing the side effects and complications of

standard treatments remains controversial because of unknown components and mechanisms [5-8]. Simple dietary supplements are also gradually being used for reducing CIT, but the evidences of effectiveness are often insufficient [9, 10]. Consequently, natural medicinal and edible plants are believed to be the best strategy to ameliorate CIT. YH0618, a medicinal and edible formula, is developed based on the theory of "medicine and food homology", ancient prescription, and a long clinical practice. The theory of "medicine and food homology" based on practice has existed in Chinese traditional medicine since ancient times [11]. It refers to that many foods are drugs and there is no absolute demarcation line between them. The medicinal foods are not only Chinese medicine with a good curative effect, but also nutritious safe food that people often eat [12].

Doxorubicin (DOX) is one of the most widely used chemotherapeutic agents and was approved for medical use in the United States in 1974 [13]. It is a class of Anthracycline Topoisomerase Inhibitor and has a broad spectrum of activity, which can be used alone and in combination with other medications. Like all chemotherapeutic drugs, DOX-induced side effects also greatly limit its clinical applications and the common side effects include alopecia, myelosuppression, vomiting, cardiotoxicity, hepatotoxicity and nephrotoxicity [14, 15]. The mechanism of DOX-mediated cytotoxicity in cancer cells is preventing DNA replication and thereby inhibiting protein synthesis [16, 17], whereas DOX-induced toxicity in normal tissues are different, including oxidative stress, downregulation of genes for contractile proteins, and apoptosis [18].

Researches have showed that antioxidants and anti-aging agents played an important role in the protection against DOX-induced toxicity [19-21]. Our pilot study showed that YH0618 decoction could reduce CIT, especially improving alopecia, skin and nail hyperpigmentation, fatigue and increasing white blood cells (WBC) through long clinical observation. These findings suggest that YH0618 had the potential effect of ameliorating DOX-induced toxicity.

As there is no scientific and systematic research exploring the effects and possible mechanism of YH0618 yet, the study aimed to evaluate whether the YH0618 would ameliorate DOX-induced toxicity mainly including alopecia, myelosuppression, cardiotoxicity, hepatotoxicity and nephrotoxicity without interfering with antitumor activity of DOX by *in vitro* and *in vivo* experiments. Besides, apoptosis in matrix cells has been proposed as the major cause of DOX-induced alopecia [22]. The mechanisms of DOX-induced myelosuppression, cardiotoxicity, hepatotoxicity and nephrotoxicity have all been

linked to apoptosis [23-25]. Apoptosis is a process of programmed cell death that occurs during embryonic development, or in maintenance of tissue homeostasis, or under pathological conditions, or in aging [26]. In apoptotic pathways, Bcl-2 and Bax are major two related proteins. Bcl-2 possesses anti-apoptotic properties and Bax is known for its pro-apoptotic function. This difference in DOX-mediated toxicity in cancer and normal cells can be investigated to improve the antitumor effects of DOX with combinatorial approaches that allow the dose reduction of DOX while protecting normal cells [27]. The shift in ratio of Bax/Bcl-2 is critical to determine the fate of a cell, apoptosis or survival. A recent study revealed that the removal of chemotherapy-induced senescent cells contributed to reducing chemotoxicity [28]. DOX could induce an upregulation of FOXO4 in senescent cells and a polypeptide FOXO4-DRI potently and selectively lowered the viability of doxorubicin-induced senescence versus control IMR90 [29]. FOXO4 is one member of the subfamily of mammalian FOXO forkhead transcription factors that are implicated to regulate a variety of processes, such as cellular proliferation, DNA repair oxidative stress and apoptosis [30, 31]. Therefore, the mechanism study was to evaluate whether YH0618 could enhance anti-apoptotic function by regulating the expressions of Bcl-2, Bax and FOXO4 in ameliorating DOX-induced toxicity.

2. Materials and Methods

2.1 Plant materials and preparation of YH0618

YH0618 consists of four medicinal foods, Sojae Semen Nigrum (Black Soybean, 30g), Brown Rice (30 g), Black Fungus (2g) and Siraitiae Fructus (1 piece), which are recommended by clinicians for cancer patients and all components have a history of safe use. All ingredients of YH0618 were from genuine producing area. Black Soybean, Brown Rice and Black Fungus were purchased from Jilin Beixian Eco Agri-industries Group Co., Ltd. (Jinlin, China). Siraitiae Fructus was purchased from Guilin Baishouyuan Food Co., Ltd. (Guangxi, China). All materials conform to Food and Environmental Hygiene Department's requirement for food safety and achieved the certificate of quality. YH0618 was baked at 130 °C and then smashed into coarse particles. 125g YH0618 coarse particles were decocted by distilled water in an electronic multipurpose health pot (BJ-33, Famous, France) three times (1:10, 1:8 and 1:8 w/v) for 30min after boiling, and then filtered with gauze and condensed by a rotary evaporator (N-1100, Hong Kong Labware Co., Ltd., Hong Kong,

China). Eventually, the condensate was dehydrated by a freeze-dryer (Ilshin BioBase Co., Ltd., Korea) and kept at -80°C (43.6 g).

2.2 UPLC determination of YH0618

UPLC analysis was performed on a Dionex Ultimate 3000 UPLC system (Sunnyvale, CA, USA) consisting of Ultimate 3000 RS Diode Array Detector (DAD), Ultimate 3000 RS Pump, Ultimate 3000 RS Autosampler, and Ultimate 3000 RS Column Compartment. Data were collected and integrated by a Chromeleon chromatogram workstation (Thermo Fisher Scientific, USA). Chromatographic separation was accomplished with an ACE Excel 2 C18 column (100 × 2.1 mm id, 1.7 μm particle size) under 35°C . The mobile phases were (A) methanol and (B) 0.1% formic acid in water. The gradient elution was applied from 1% to 90% of Solvent A starting from 0 to 27 min and the flow rate was 0.3 mL/min. Certain amounts of individual standards daidzin, daidzein, genistin and genistein (purchased from Sichuan Weikeqi Biological Technology Co., Ltd.) were dissolved in 80% methanol together to compose the mixed standard solution (daidzin 1.15 mg/mL, daidzein 1.2 mg/mL, genistin 1.1 mg/mL and genistein 1.15 mg/mL). YH0618 sample and the mixed standard solution were filtered through a 0.22 μm PTFE syringe filter (Millipore, Bedford, MA, USA). The injection volume was 5 mL and DAD detection was set at 260 nm.

2.3 Cell lines and cell culture

Human breast cancer cell lines MDA-MB-231 and MCF-7 cells, human normal liver L02 cells, human normal Human Embryonic Kidney 293 (HEK-293) cells were purchased from the American Type Culture Collection and cultured in medium (DMEM for MCF-7 and HEK-293; RPMI-1640 for MDA-MB-231 and L02) added with 10% FBS and 1% penicillin and streptomycin (Gibco Life Technologies, Lofer, Austria) at 37°C in a humidified incubator.

2.4 Cell proliferation assay

The effects of YH0618 with or without DOX on cancer cell proliferation were detected by cell viability, as determined by MTT assay. The concentration of YH0618 (from 6.25 to 100 $\mu\text{g}/\text{ml}$) was determined by pre-culturing the MDA-MB-231, MCF-7, L02 and HEK-293 cells with different concentrations of YH0618 at 5, 25, 50, 100, 200 and 400 $\mu\text{g}/\text{ml}$, respectively. The optimal concentrations were chosen as 100 $\mu\text{g}/\text{ml}$ was the highest concentration at which the normal liver and kidney cells survived well. In brief, MDA-MB-231, MCF-7, L02 and HEK-293 cells were planted in 96-well plates at a density of 5×10^3 cells per well. After serum starvation, DOX, YH0618 or YH0618 with DOX at IC50

concentrations were added to the wells, with six repeats for each concentration. Cell proliferation at 48h was then evaluated by MTT according to the manufacturer's instructions. A triplicate independent experiment was conducted. The surviving cells converted MTT to formazan that generates a blue-purple color when dissolved in DMSO that was measured at 540 nm using a model 680 Microplate Reader (Bio-Rad Laboratories, Hercules, CA, USA). The relative percentage of cell survival was calculated by dividing the absorbance of treated cells by the control in each experiment.

2.5 Flow cytometry analysis

Apoptosis was detected by Annexin V-fluorescein isothiocyanate (FITC)/ propidium iodide (PI) double staining and flow cytometry analysis. MDA-MB-231, MCF-7, L02 and HEK-293 cells were incubated with DOX at IC50 concentrations, YH0618 (25, 50, 100 $\mu\text{g}/\text{mL}$), and YH0618 with DOX for 16h, and then harvested and resuspended in PBS. Apoptotic cells were determined by Annexin V-FITC Apoptosis Detection kit (Sigma, St. Louis, MO) according to the manufacturer's instructions. Percentages of apoptosis cells were determined by BD FACSCantoII Analyzer (BD Biosciences, San Jose, CA).

2.6 Western blot analysis

MDA-MB-231, MCF-7, L02 and HEK-293 cells were lysed in RIPA buffer (Sigma, St. Louis, MO) containing a protease inhibitor mixture (Roche Diagnostics, IN), and the protein concentration was measured with the bicinchoninic acid assay (Thermo Fisher Scientific, Bonn, Germany). Quantified protein lysates (30 μg) were subjected to sodium dodecyl sulfate polyacrylamide gel electrophoresis (SDS-PAGE) and resolved on 12% polyacrylamide gels. The proteins were then transferred onto a PVDF membrane (GE Healthcare, Freiburg, Germany). The membranes were blocked with 5% (w/v) non-fat milk powder in TBS with 0.1% (v/v) Tween-20 for 1h at room temperature, followed by incubation with primary antibodies, including Bax, Bcl-2 and FOXO4 (Gene Co., Ltd., Tokyo, Japan) at 4°C overnight. Then the membrane was incubated with corresponding secondary anti-mouse or anti-rabbit antibodies (Gene Co., Ltd., Tokyo, Japan) for 1 h at room temperature. The signals were visualized using the ECL Advance reagent (GE Healthcare) and quantified using Quantity One software.

2.7 Animal models

MMTV-PyMT(+/-) female mice were used to evaluate whether YH0618 affected the anti-cancer activities of DOX. MMTV-PyMT mice are

internationally accredited models used for investigating mammary carcinogenesis, which can spontaneously produce luminal-like breast tumor and recapitulate similar pathological processes and characteristics found in human breast cancer [32]. MMTV-PyMT (+/-) female mice were randomly divided into the following groups: (a) tumor control group; (b) DOX (5 mg/kg) alone; (c) YH0618 (4.5 g/kg) alone; and (d) doxorubicin (5 mg/kg) + YH0618 (4.5 g/kg). The daily intake of YH0618 in the human was 62.5g, so usually 9 g/kg mice weight of YH0618 should be the middle dosage in this study according to the dose conversion method between mice and human. However, our pilot study revealed that the medium dosage 9 g/kg was too high to induce mass mice deaths, therefore, the low dosage 4.5 g/kg was chosen as the optimal concentration. Each group included 9 animals; (a) and (c) group received intraperitoneal injection of 0.2 ml vehicle alone and others received 0.2 ml DOX respectively once a week for 3 weeks. Besides, (c) and (d) mice received YH0618 by intragastric administration every day, while (a) and (b) mice received 0.9% NaCl in the same way for 3 weeks. Mice body weights were measured every 4 days. After 3 weeks of intervention, all mice were anesthetized and killed. Tumor volume and weight were measured. The blood, heart, liver, kidney, lung and tumor were collected, and then WBC and red blood cells (RBC) were counted; Alanine aminotransferase (ALT), aspartate aminotransferase (AST), blood urea nitrogen (BUN) and creatinine in whole blood were measured by kits. All tissues were conducted histopathology examination.

C57BL/6 mice were used to explore the role of YH0618 in improving DOX-induced alopecia and skin pigmentation. The specific method was as described by Paus [33]. The dorsal skin of 7-week-old C57BL/6 mice was treated with a depilatory cream. Then all the hair shafts were removed and the homogeneous pink skin color of the skin revealed the telogen phase of the hairs. Depilation at this hair stage induced the development of a synchronous anagen stage. The grouping and administration methods were as above except that the start time of administration was exactly 9 days after depilation when synchronized hair follicles were in the anagen VI phase. Hair and skin color were recorded every week after treatment. After 3 weeks of treatment, all mice were anesthetized and killed, and the skin was collected. The hair follicles were studied on paraffin sections stained with hematoxylin-eosin staining.

All animal experiments complied with the ARRIVE guidelines and were carried out in accordance with the National Institutes of Health guide for the care and use of Laboratory animals.

Besides, these experiments were approved by the Committee on the Use of Live Animals in Teaching and Research of the University of Hong Kong (CULATR 3769-15).

2.8 Blood test

Blood samples for WBCs and RBCs counts (no more than 10% of total volume) were collected in 100 μ l EDTA-coated tubes. The tubes swirled for about 60 seconds to ensure all EDTA was mixed well with the blood. Analysis was performed as soon as possible after blood collection. RBCs and WBCs were observed using a haemocytometer under a microscope, and when counting WBCs, the blood need to be dealt with 3% acetic acid. ALT, AST, BUN and creatinine activities were determined under the manufacturer's instruction (Biovision US). All samples were analyzed within two days upon collection.

2.9 Histopathology

All tissue samples were fixed in 10% paraformaldehyde/PBS for 24h, and then dehydrated in ethanol, cleared by xylene and embedded in 4% paraffin at 4°C, and then sectioned (5 μ m). Deparaffinized tissues were stained with hematoxylin and eosin. The slides were observed under a microscope (Olympus BX43, Tokyo, Japan).

2.10 Statistical Analysis

The data were shown as the mean \pm SD. A two-tailed one-way analysis of variance (ANOVA) was used to determine the significance of the data between groups. Statistical significance was reached when the *P* value <0.05.

3. Results

3.1 Determination of main components from YH0618

The established UPLC method proved to be simple, linear, precise, accurate, stable, repeatable and rapid (data were not showed). The main components of YH0618 were successfully determined. As shown in Figure 1, daidzin, daidzein, genistin and genistein were identified by retention time on the analytical system.

3.2 YH0618 selectively inhibited DOX cytotoxicity in normal liver and kidney cells but not in breast cancer cells.

Cultures were initially exposed to DOX at doses from 0 μ M to 10 μ M to determine the IC₅₀ value on MDA-MB-231, MCF-7, L02 and HEK-293 cells. After 48 h, a dose-dependent reduction in all cells viability (IC₅₀ value of MDA-MB-231 cells = 1.6 μ M, MCF-7 cells=2.2 μ M, L02 cells=6 μ M, HEK-293 cells=6 μ M)

was observed (Figure 2A). Then we observed the effects of YH0618 at doses from 6.25 $\mu\text{g}/\text{ml}$ to 100 $\mu\text{g}/\text{ml}$ on all cancer and normal cells. The results after 48h showed that YH0618 inhibited the breast cancer cells growth at high concentrations, while promoted normal liver and kidney cells growth (Figure 2B, F value in MDA-MB-231 cells = 74.92, MCF-7 cells=36.82, L02 cells=15.63, HEK-293 cells=11.38). In order to evaluate the effect of YH0618 on DOX-induced cytotoxicity, we selected YH0618 at doses of 6.25 $\mu\text{g}/\text{ml}$ to 100 $\mu\text{g}/\text{ml}$ for DOX at IC50 value combination studies. YH0618 did not affect the DOX-induced cancer cell death, but high doses reduced DOX-induced growth inhibition in the normal liver and kidney cells (Figure 2C, F value in MDA-MB-231 cells = 38.48, MCF-7 cells=26.77, L02 cells=100.02, HEK-293 cells=58.66), suggesting that YH0618 might protect DOX-induced the hepatotoxicity and nephrotoxicity without interfering with its anti-cancer effects.

3.3 YH0618 selectively inhibited DOX-induced apoptosis in normal liver and kidney cells but promoted the apoptosis in breast cancer cells

Annexin V/PI staining was performed to investigate whether or not DOX-induced cell death in breast cells, and normal liver and kidney cells through apoptosis. Staining with Annexin V is typically used in conjunction with a vital dye such as propidium iodide (PI) for identification of early and late apoptotic cells. Viable cells with intact membranes exclude PI, whereas the membranes of dead and damaged cells are permeable to PI [34]. Therefore, both Annexin V and PI negative represent viable cells,

while Annexin V positive and PI negative cells indicate early apoptosis, and both Annexin V and PI positive cells indicate late apoptosis. Dead cells are Annexin V negative and PI positive. DOX (IC50) treatment induced apoptosis in 23% of the MCF-7 cells, 30% of the MDA-MB-231 cells, 19% of the L02 cells, and 8% of the HEK-293 cells, respectively. The percentage of YH0618-induced apoptosis alone in MDA-MB-231 and MCF-7 were 10%-20%. However, YH0618 did not induce apoptosis in L02 and HEK-293 cells. The co-treatment of DOX and YH0618 increased the percentage of DOX-induced apoptosis in breast cancer cells, but reduced in L02 and HEK-293 cells, suggesting that YH0618 protected DOX-induced apoptosis in normal cells (Figure 3,4).

3.4 YH0618 attenuated DOX-induced apoptosis in normal liver and kidney cells through FOXO4-mediated (Bcl-2 family members) mechanism

In vitro evidence demonstrated that DOX caused hepatotoxicity and nephrotoxicity by cell apoptosis and YH0618 could attenuate the apoptosis in normal liver and kidney cells. FOXO4 can trigger apoptosis by modulating the ratio of proapoptotic and prosurvival members of the Bcl-2 family. Thus we further explored the possible mechanism through FOXO4-mediated Bcl-2 family members in L02 and HEK293 cells. As shown in Figure 5 and Figure 6, for both L02 and HEK293 cells, the ratio of Bax/Bcl-2, and level of FOXO4 were increased in DOX group. These changes were attenuated significantly in DOX (6 μM)+ YH0618 (100 $\mu\text{g}/\text{ml}$) group.

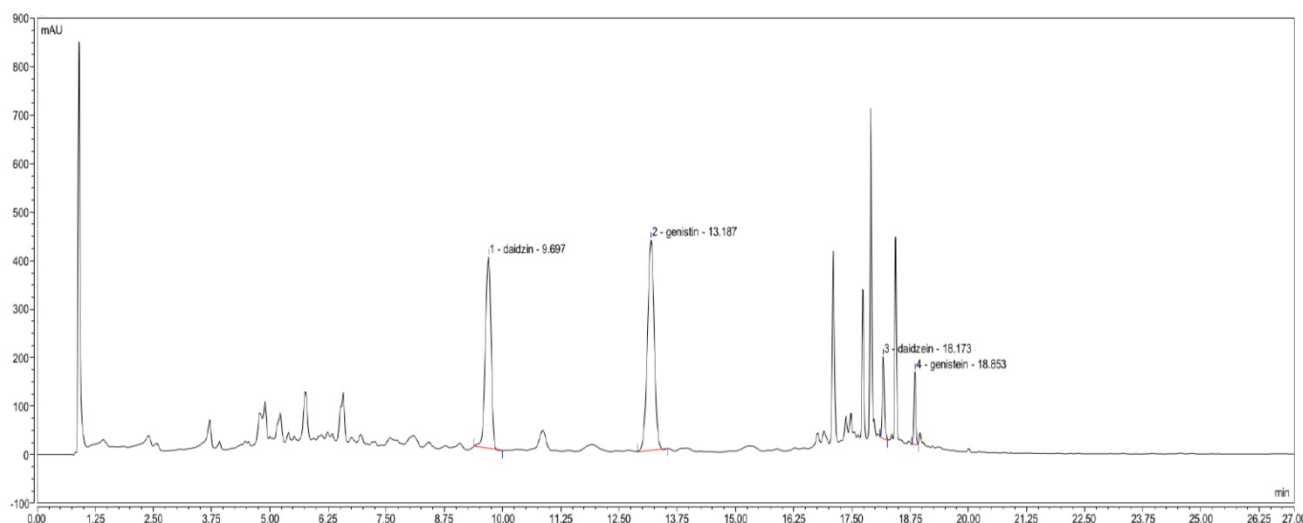


Figure 1. UPLC determination of YH0618. In the UPLC fingerprint at an absorbance of 260 nm, the peaks corresponding to daidzin, daidzein, genistin and genistein were identified.

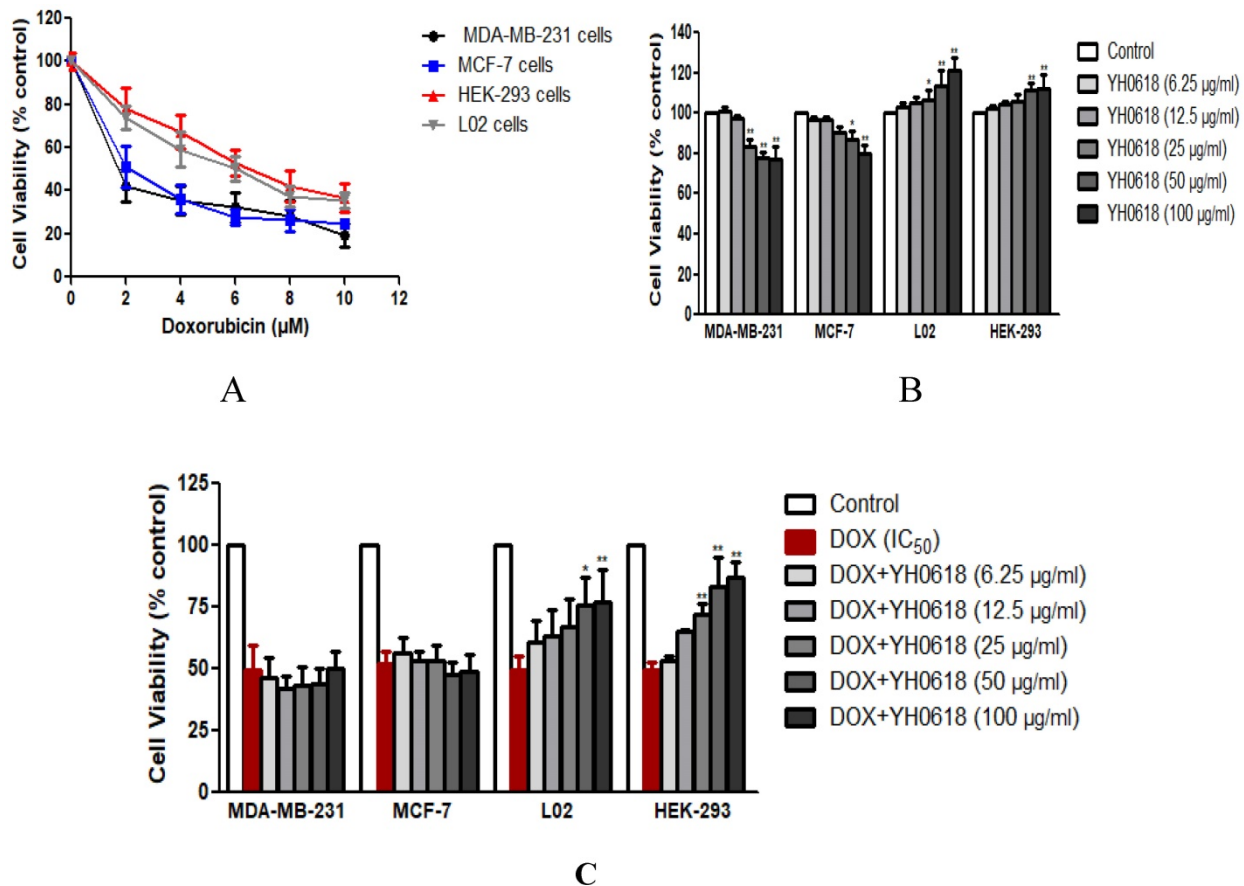


Figure 2. YH0618 selectively inhibited DOX cytotoxicity in normal liver and kidney cells but not in breast cancer cells. (A) MDA-MB-231, MCF-7, L02 and HEK-293 cells were treated with various concentrations (0 µM to 10 µM) of DOX for 48 h to determine the IC₅₀ value of DOX on these cells by MTT assay. Data were represented as a percentage of the vehicle-treated control. (B) MDA-MB-231, MCF-7, L02 and HEK-293 cells were incubated with YH0618 (6.25 µg/ml to 100 µg/ml) for 48 h and subjected to an MTT assay to determine the proliferation rate. (C) The MDA-MB-231, MCF-7, L02 and HEK-293 cells were incubated with DOX (IC₅₀ value) and YH0618 (6.25 µg/ml to 100 µg/ml) for 48 h, and then subjected to an MTT assay. Data were represented as a percentage of the vehicle-treated control. **P*<0.05, ***P*<0.01 vs. DOX control

3.5 YH0618 potentiated the effect of DOX-induced anti-cancer and significantly reduced DOX-induced hair loss

The effect of YH0618 on reducing DOX-induced hepatotoxicity and nephrotoxicity without interfering with its anti-cancer effects in vitro experiment was validated in this study. Hence, we evaluated whether or not YH0618 affected the antitumor effect of DOX in MMTV-PyMT(+/-) female mice. The results showed that DOX significantly reduced the body weight compared to control group, but YH0618 did not reduce the body weight (Figure 7A). At the end of the experiment, both DOX and YH0618 alone treatment significantly reduced the tumor volumes (DOX: 402.5 mm³, YH0618: 650 mm³) compared with the control group (1644 mm³). A significant decrease in the tumor volume of the co-administration was observed (Figure 7B).

As the clinical trial presented that YH0618 could significantly improve chemotherapy-induced alopecia, we further demonstrated the efficacy in the 7-week-old C57BL/6 mice. The Figure 8 showed the visualized and histopathological evidence that DOX

reduced the hair follicle, and damaged sebaceous gland and piloerector muscle, but YH0618 improved the conditions.

3.6 YH0618 improved WBC and RBC, and protected DOX-induced heart, liver and kidney damage

Considering in vitro observations that YH0618 could decrease DOX cytotoxicity in normal liver and kidney cells, we further investigated its effect on DOX-induced organs damage in vivo experiment. MMTV-PyMT(+/-) female mice were treated with DOX at 5 mg/kg (i.p.) for 3 weeks that may cause chronic toxicity. The DOX-induced myelosuppression, hepatotoxicity and nephrotoxicity were clearly revealed by the reduction of WBC and RBC, and the increase in serum biochemical markers, particularly ALT, AST, BUN and creatinine. DOX treatment resulted in a significant decrease in WBC and RBC, and increase in ALT and AST, respectively, compared with the control group. YH0618 supplementation alone did not exhibit significant changes in the biochemical markers. Conversely, the

co-treatment of DOX and YH0618 resulted in a partial reversal of DOX-induced decrease in WBC and RBC, and the increase in ALT and AST (Table 1 and 2).

Table 1. Effect of YH0618 on WBC and RBC in peripheral blood of MMTV-PyMT(+/-) female mice

Group	WBC (10 ⁹ /L)	RBC(10 ¹² /L)
Tumor control	5.74 ± 0.4	10.95 ± 0.61
DOX alone (5 mg/kg)	1.32 ± 0.37*	6.28 ± 0.76*
YH0618 alone (4.5 g/kg)	5.85 ± 0.74	10.45 ± 1.04
DOX (5 mg/kg)+YH0618 (4.5 g/kg)	1.39 ± 0.18*	6.83 ± 0.61*

*P<0.05 vs. tumor control

Table 2. Effect of YH0618 on ALT, AST, BUN and creatinine in peripheral blood of MMTV-PyMT(+/-) female mice

Group	ALT(U/L)	AST(U/L)	BUN(mg/dL)	Creatinine(mg/dL)
Tumor control	40.80±15.71	105.29±14.32	38.55±5.21	0.17±0.02
DOX alone (5 mg/kg)	72.96±3.73*	156.11±17.36*	46.15±6.73	0.27±0.01
YH0618 alone(4.5 g/kg)	32.82±6.81	116.13±18.38	35.70±5.73	0.14±0.01
DOX (5 mg/kg)+YH0618 (4.5 g/kg)	57.16±11.03#	169.03±20.8	45.25±4.83	0.19±0.01*

*P<0.05 vs. tumor control. #P<0.05 vs. tumor control.

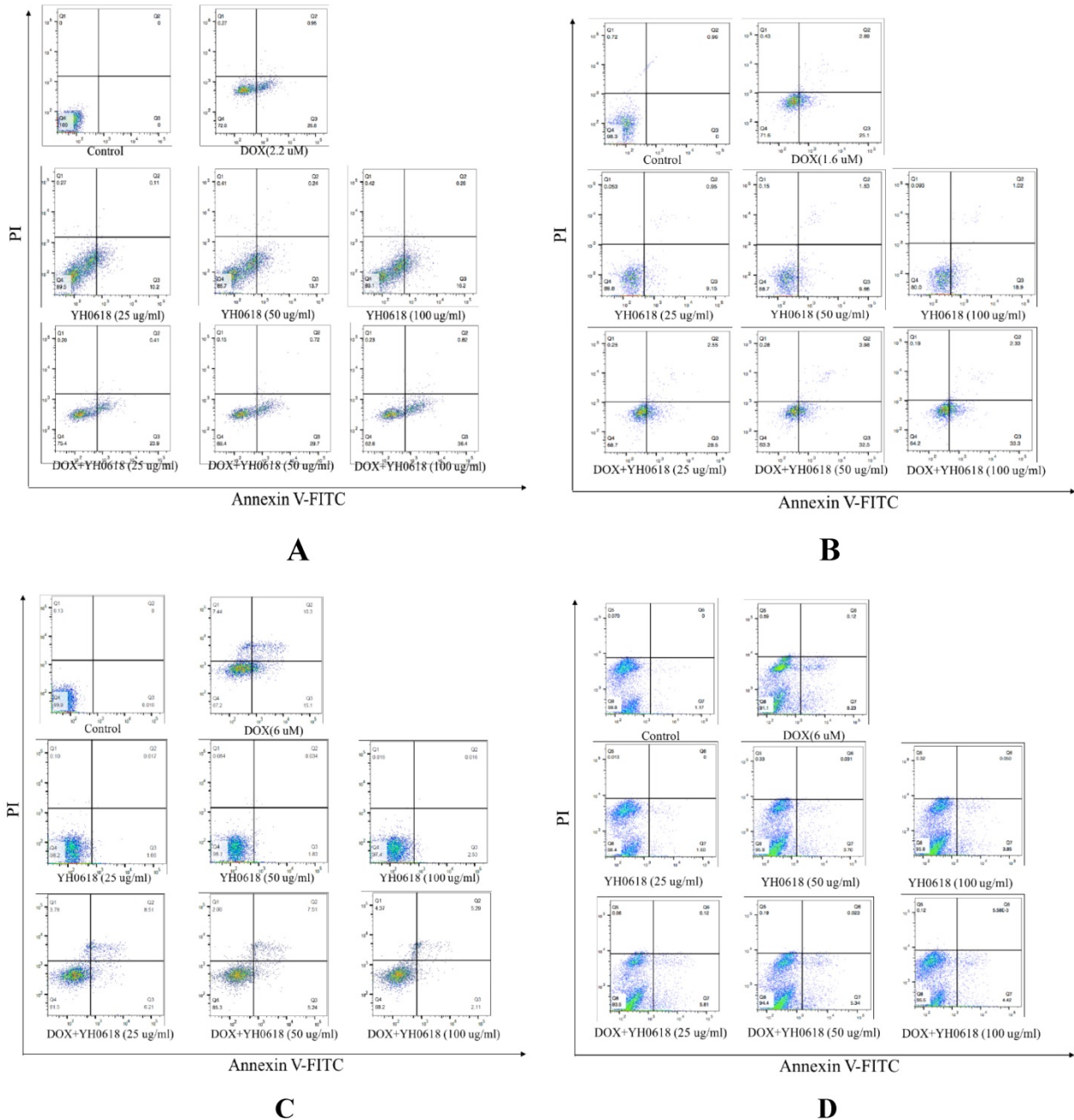


Figure 3. YH0618 potentiated the effect of DOX on apoptosis in breast cancer MCF-7 cells and MDA-MB-231 cells, but suppressed the effect of DOX on apoptosis in normal liver L02 cells and kidney HEK293 cells. All cells were incubated with DOX (IC₅₀) and/or YH0618 (25, 50 and 100 µg/ml) for 16 h, and then analyzed by flow cytometry using Annexin V/PI staining to discriminate the live cells (Q4), early apoptotic cells (Q3), necrosis or late apoptotic cells (Q2), and dead cells (Q1). (A) MCF-7 cells were incubated with DOX (2.2 µM) and/or YH0618. (B) MDA-MB-231 cells were incubated with DOX (1.6 µM) and/or YH0618. (C) L02 cells were incubated with DOX (6 µM) and/or YH0618. (D) HEK-293 cells were incubated with DOX (6 µM) and/or YH0618.

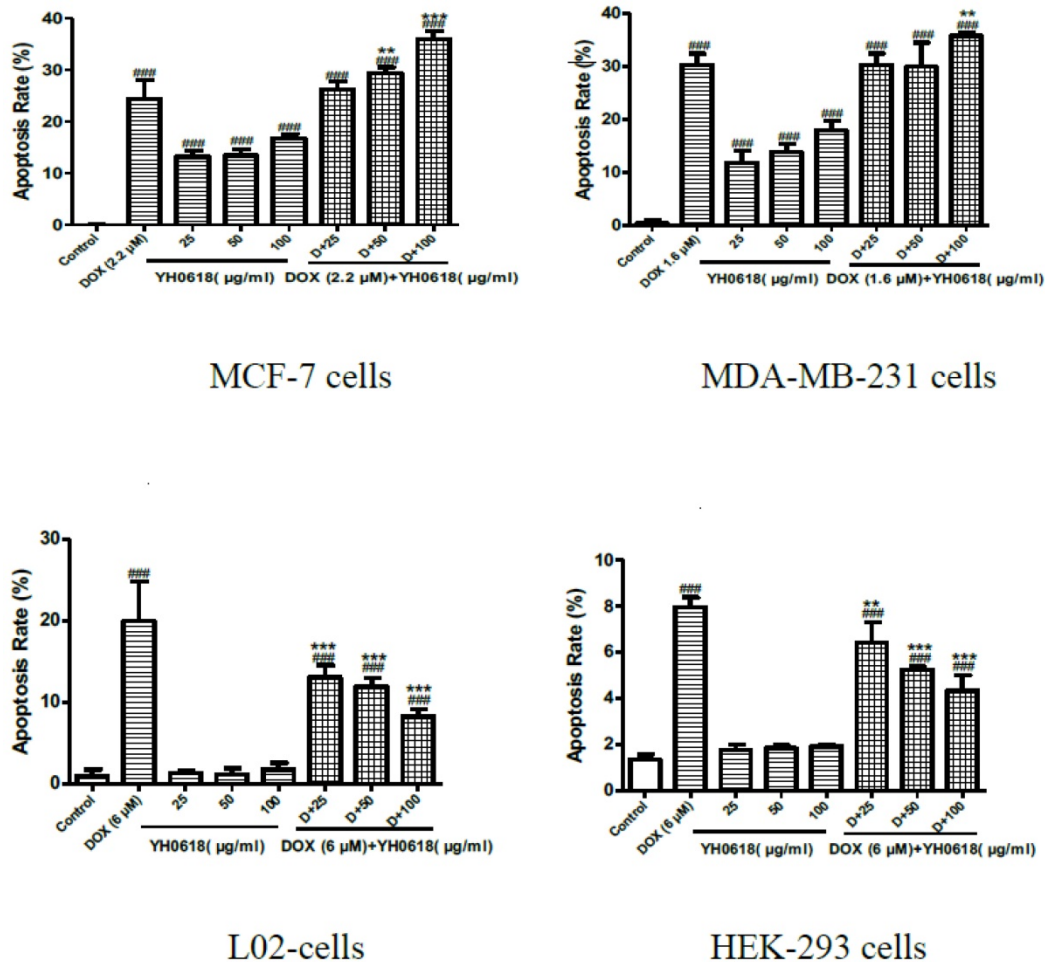


Figure 4. YH0618 selectively inhibited DOX-induced apoptosis in normal liver and kidney cells but increased the apoptosis in breast cancer cells. Data were presented as a percentage of the vehicle-treated control. ### $P < 0.001$ vs. Control; *** $P < 0.001$, ** $P < 0.01$ presented DOX+ YH0618 vs. DOX

The microscopic examination revealed that the control and YH0618-treated hepatic tissues have large normal polygonal cells with prominent round nuclei and eosinophilic cytoplasm, as well as a few spaced hepatic sinusoids arranged in-between the hepatic cords. By contrast, the mice that received DOX showed massive hepatotoxicity, with the dissolution of involved hepatic cords, which appeared as empty vacuoles aligned by strands of necrotic hepatocytes and kupffer cells proliferated in a diffused manner between the fatty degenerated hepatocytes (Figure 9A). For kidney tissue, control and YH0618 groups showed normal renal glomeruli and cortical tubules structures. However, DOX-treated group displayed glomeruli distortion, filtration space obliterated disappear, tubules focal atrophy necrosis and exfoliation, and vascular congestion (Figure 9B). Besides, DOX caused cytoplasmic vacuolization, mitochondrial swelling, and cristae disappearance, while control and YH0618-treated group showed normal heart ultrastructure (Figure 9C). These hepatic, cardiac and renal damage after DOX treatment could be significantly reduced upon

co-treatment with YH0618. Histopathological evidence also revealed that DOX inhibited the pulmonary metastasis of breast cancer cells and no significant lung damages were showed in all groups (Figure 9D).

Discussion

Although DOX is the most commonly used anticancer drug, its clinical use is limited by its toxicity to normal tissues, such as the heart, liver and kidney. As evidence of effective intervention in reducing DOX-induced toxicity for cancer patients is scant and the managements are lack of clinical efficacy and even cause some other side effects, medicinal food is believed to be a successful measure for detoxification and YH0618 was developed. In the YH0618 prescription, black soybean is the main essential ingredient and has been used for detoxification over the millennia in China. *In vitro* and *in vivo* models, black soybean has been proved to be the quite safe medical food [35]. Our result showed that DOX inhibited the proliferation in breast cancer MCF-7 and MDA-MA-231cells, and the IC50 value

were 2.2 μ M and 1.6 μ M, respectively. Besides, DOX also induced cytotoxicity in L02 cells and HEK-293 cells, and both the IC50 values were 6 μ M. The results were consistent with previous studies. The co-treatment of YH0618 and DOX significantly attenuated DOX-induced growth inhibition in L02 and HEK-293 cells, and simultaneously potentiated the antitumor effects of DOX in human breast cancer cells.

DOX is known to interact with DNA by intercalation to inhibit the role of the enzyme topoisomerase II during transcription and replication [36]. Although the exact mechanism of DOX-induced cytotoxicity remains unknown, it is believed to be mediated through free radical formation, oxidative damage, and apoptosis [37]. DOX-induced apoptosis is associated with two distinct pathways, including

the death receptor pathway and the mitochondrial pathway. The mitochondrial pathway is the major mechanism of DOX-induced apoptosis. The mitochondria are not only involved in caspase-dependent apoptosis, but also significantly affect the Bcl-2 pathway during caspase-independent apoptosis [38]. Mitochondrial alterations are one of the main pathways regulating Bcl family proteins and caspase-independent apoptosis, in which Bcl-2 (an anti-apoptotic factor) and Bax (a pro-apoptotic factor) play key roles in regulating the effect of mitochondrial membrane permeability, mitochondrial function and Cyt-c release. Thus, our study observed the effect of DOX or/and YH0618 on apoptosis and the results showed that YH0618 selectively inhibited DOX-induced apoptosis in normal liver and kidney cells but promoted the apoptosis in breast cancer cells.

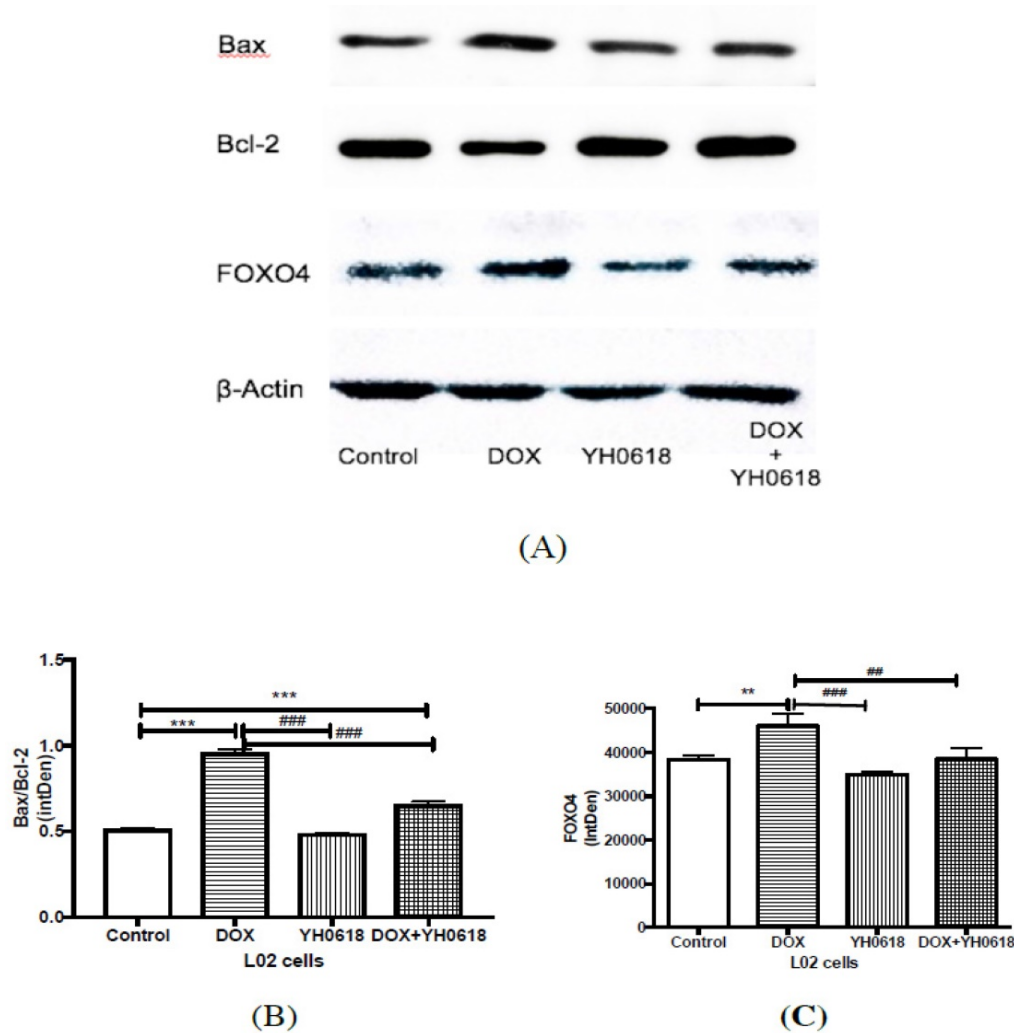


Figure 5. Apoptosis related protein expressions were determined by western blot analysis in DOX and/or YH0618-treated L02 cells. (A, B) The ratio of Bax/Bcl-2 was increased significantly in DOX group versus control group, which was recovered in DOX (6 μ M)+ YH0618 (100 μ g/ml) group in L02 cells. (A, C) The increased level of FOXO4 was shown in DOX group versus control group, which was attenuated in DOX + YH0618 group in L02 cells (F=26.77). *P<0.05, **P<0.01, ***P<0.001 vs. control group; #P<0.05, ##P<0.01, ###P<0.001 presented vs. DOX group.

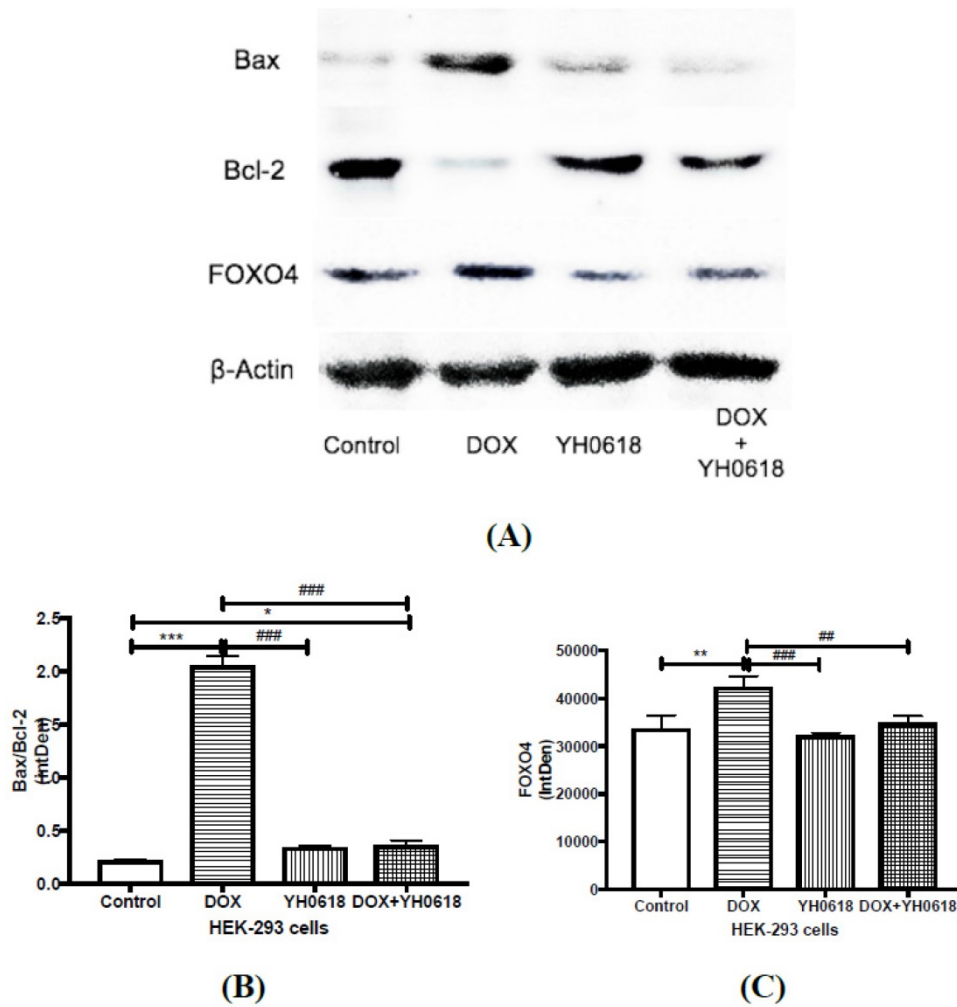


Figure 6. Apoptosis related protein expressions were determined by Western blot analysis in DOX and/or YH0618-treated HEK-293 cells. (A, B) The ratio of Bax/Bcl-2 was increased significantly in DOX group versus control group, which was recovered in DOX (6 μ M)+ YH0618 (100 μ g/ml) group in HEK293 cells. (A, C) The increased level of FOXO4 was shown in DOX group versus control group, which was attenuated in DOX + YH0618 group in HEK-293 cells (F=38.66). *P<0.05, **P<0.01, ***P<0.001 vs. control group; ###P<0.01, ####P<0.001 presented vs. DOX group.

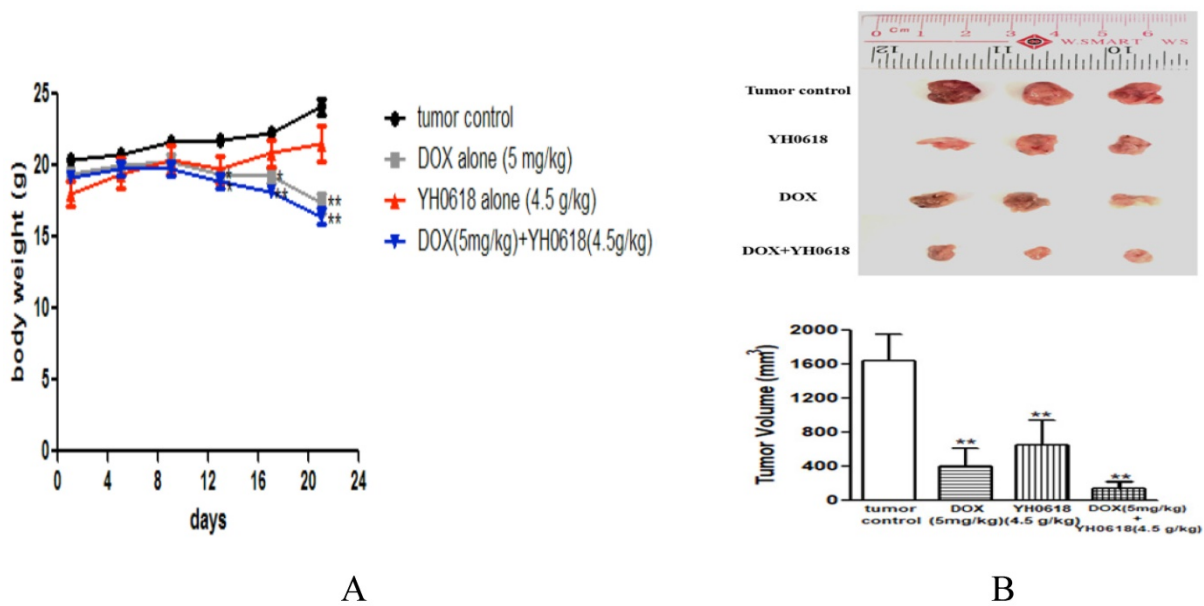


Figure 7. The effect of YH0618 on body weight and tumor in mice. (A) The body weights between control and YH0618-treated group had little differences. All values represented as means \pm SD, n = 9, * P < 0.05, ** P<0.01 vs. tumor control. (B) At the end of three weeks, the tumors were collected and weighed. DOX and YH0618 alone treatment reduced the tumor size compared with the control groups (**P<0.01). Co-treatment significantly reduced the tumor size compared with other treatment groups (F=65.27,**P<0.01). ** P<0.01 vs. tumor control.

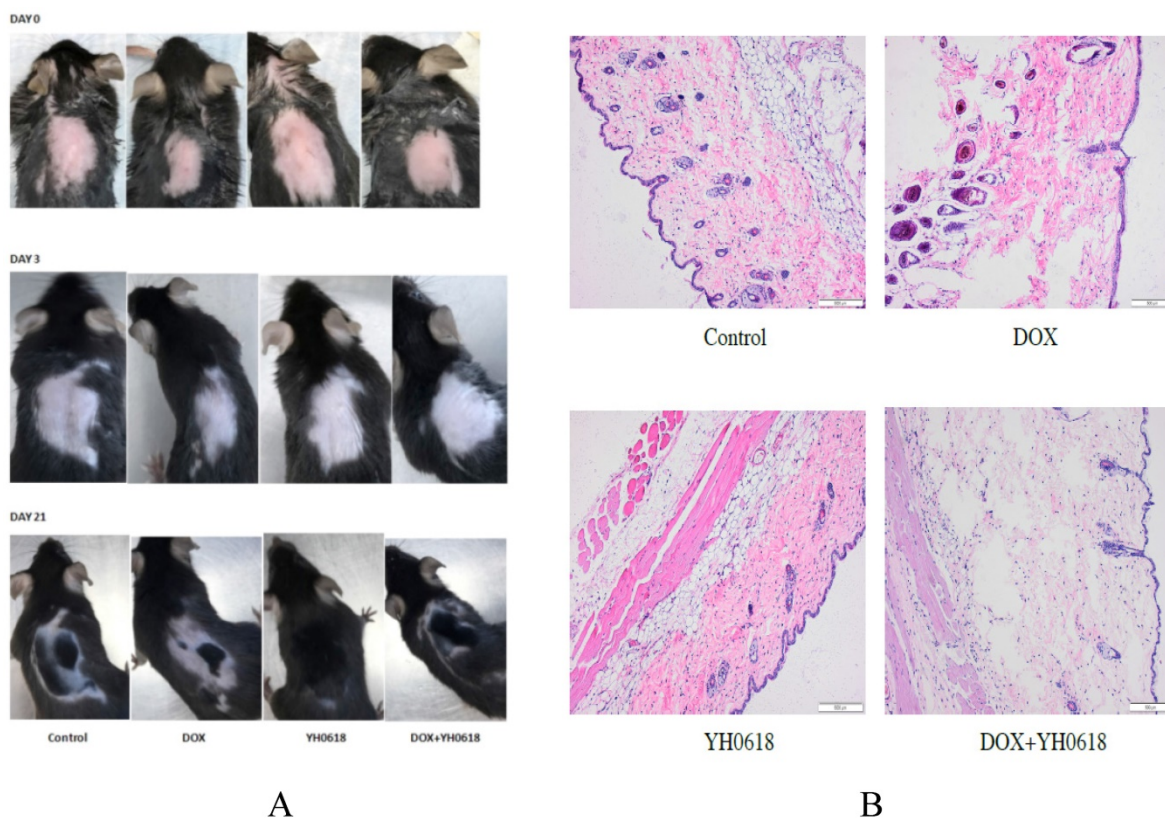


Figure 8. YH0618 significantly reduced DOX-induced hair loss. (A) The visualized appearance of alopecia in 7-week-old C57BL/6 mice at day 0, 3 and 21 after administration of DOX (5 mg/kg) and/or YH0618 (4.5 g/kg). (B) Histopathological appearance of the skin collected, at the end of the experiment, from the C57BL/6 mice. DOX reduced the hair follicle, and damaged sebaceous gland and piloerector muscle, but YH0618 improved the conditions.

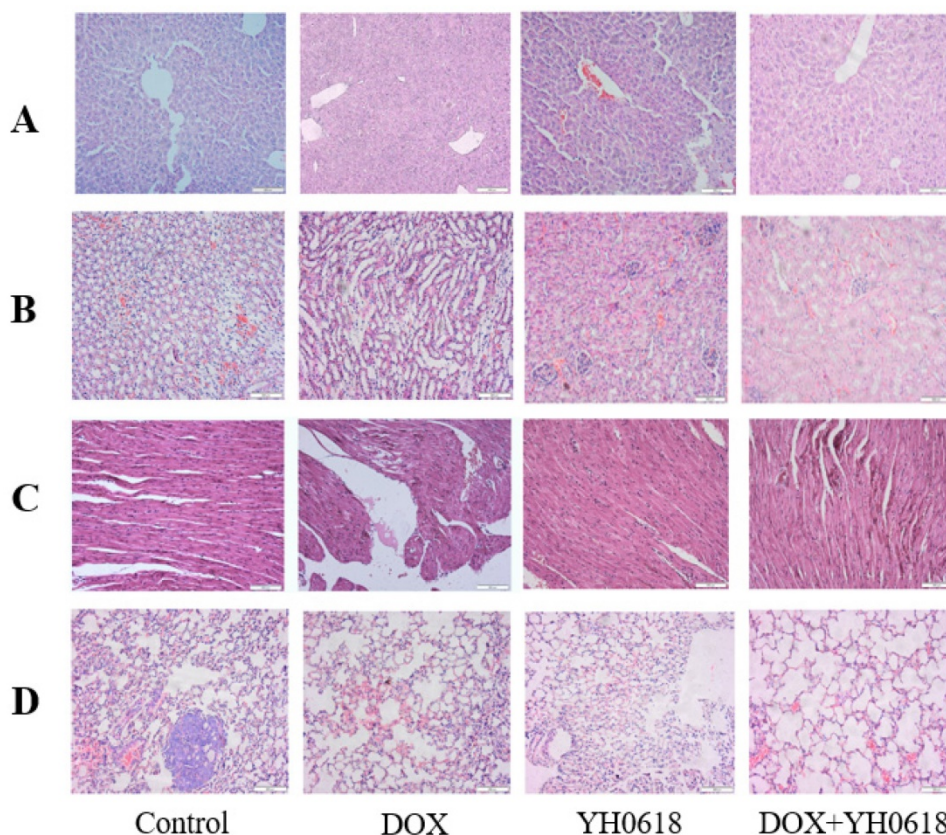


Figure 9. Histological changes in the MMTV-PyMT (+/-) female mice liver, kidney, heart and lung that received DOX (5 mg/kg) and/or YH0618 (4.5 g/kg). The histopathological appearance of liver (A), kidney (B), heart (C) and lung (D) collected, at the end of the 21 day after administration of DOX (5 mg/kg) and/or YH0618 (4.5 g/kg).

A recent study revealed that the removal of chemotherapy-induced senescent cells contributed to reducing CIT. DOX could induce an upregulation of FOXO4 in senescent cells and a polypeptide FOXO4-DRI potently and selectively lowered the viability of doxorubicin-senescent versus control IMR90 [21]. In addition, FOXO factors can also cause apoptosis by modulating the ratio of proapoptotic and prosurvival members of the Bcl-2 family. This study also demonstrated that DOX induced that upregulation of FOXO4 protein and Bax/Bcl-2 in normal liver and kidney cells, but they were attenuated by co-administration with YH0618. The possible reason is that DOX triggers senescence in L02 and HEK-293 cells, with elevated FOXO4 activity and YH0618 directly interacted with FOXO4 or killed senescent cells to decrease the Bax/Bcl-2, preventing the apoptosis.

DOX can cause different side-effects such as cardiotoxicity, nephrotoxicity, hepatotoxicity and cutaneous injuries as a result of multidirectional cytotoxic effects. And the severity of these side-effects mainly depends on the dosage of DOX. Previous study showed that some supplement like Vitamin B6, medecassoside could prevent DOX-induced toxicity in animals [37, 39]. We also confirmed that the medical food YH0618 protected DOX-induced heart, liver and kidney injury in mice. The data also demonstrated that long administration of DOX reduced WBC and RBC, and increased serum indices of liver function, including ALT and AST. Interestingly, YH0618 partially reversed DOX-induced decrease in WBC and RBC, and increase in ALT. WBC counts are often regarded as indicators of many diseases. During chemotherapy, the decrease of WBC counts in peripheral blood not only lead to fever, even septicemia and in severe cases, bleeding, which is one of the reasons of complications after chemotherapy, but also disturb the process of chemotherapy, further reducing the efficacy of treatments [40]. RBC are the most common type of blood cell and can deliver oxygen to the body tissues. Its decrease may result in anemia and the symptoms include shortness of breath, palpitation of the heart and fatigability [41]. Studies showed that chemotherapy-induced high levels of ALT and AST were attributed to the hepatocellular damage and decreased liver functions [42].

The effect of YH0618 on alopecia was also observed in the 7-week-old C57BL/6 mice. The mechanism of chemotherapy-induced alopecia have been explored by many researchers, mainly including mitosis interruption, impairment of metabolic processes, and hair matrix cell apoptosis [43]. In which P53-dependent apoptosis of hair-matrix

keratinocytes and chemotherapy-induced hair-cycle abnormalities plays an important role in the occurrence of alopecia and hair-regrowth [44]. In this study, the appearances and histopathological evidence showed that DOX reduced the hair follicle, and damaged sebaceous gland and piloerector muscle, but YH0618 reversed the conditions.

Conclusion

In summary, the present findings demonstrated that YH0618 selectively attenuated the toxic effects of DOX in normal tissues, and simultaneously potentiated the anti-cancer effect of DOX by apoptosis pathways. The results suggest that YH0618 may serve as a valuable protective agent in chemotherapy-induced toxicity. Furthermore, this different effects caused by YH0618 in cancer and normal cells could be investigated to improve the antitumor effects of DOX with combinatorial approaches that allow the dose reduction of DOX while protecting normal cells. Nowadays, healthy products developed by medicinal and edible plants are more scientific and rational than drug, and the development and utilization will have broader market.

Abbreviations

CIT: chemotherapy-induced toxicity; DOX: doxorubicin; WBC: white blood cells; RBC: red blood cells; SDS-PAGE: sodium dodecyl sulfate polyacrylamide gel electrophoresis; ALT: alanine aminotransferase; AST: Aspartate aminotransferase; BUN: blood urea nitrogen; PI: propidium iodide.

Acknowledgements

We express our most sincere gratitude to all the professionals who selflessly participated in this study.

Funding

This work was supported by the Seed Fund for Translational and Applied Research from HKU (201611160019), Innovation and Technology Fund from Hong Kong government (UIM/276) and China Postdoctoral Science Foundation (2018M633037).

Competing Interests

The authors have declared that no competing interest exists.

References

1. Chabner BA, Roberts TG Jr. Timeline: Chemotherapy and the war on cancer. *Nat Rev Cancer*. 2005; 5: 65-72.
2. Nakamura Y, Momokawa K, Sasaki T, et al. Effect of steroid on antiemetic for side effect of anticancer chemotherapy. *Gan To Kagaku Ryoho*. 2005; 32: 401-4.
3. Saxena A. Cancer chemotherapy and its side effect management. *Nurs J India*. 2006; 97: 109-10.

4. Schumacher K. Effect of selenium on the side effect profile of adjuvant chemotherapy/radiotherapy in patients with breast carcinoma. Design for a clinical study. *Med Klin (Munich)*. 1999; 94: 45-8.
5. Chao J, Dai YT, Verpoorte R, et al. Major achievements of evidence-based traditional Chinese medicine in treating major diseases. *Biochem Pharmacol*. 2017; 139: 94-104.
6. Bonan H, Rui L, Zhen Q, et al. Oral Chinese herbal medicine as an adjuvant treatment for chemotherapy, or radiotherapy, induced myelosuppression: A systematic review and meta-Analysis of randomized controlled trials[J]. *Evid-Based Compl and Alt Med*. 2017; 2017:1-13.
7. Jia YJ, Du HH, Yao M, et al. Chinese herbal medicine for myelosuppression induced by chemotherapy or radiotherapy: a systematic review of randomized controlled trials. *Evid Based Complement Alternat Med*. 2015; 2015: 1-12.
8. Yin SY, Wei WC, Jian FY, et al. Therapeutic applications of herbal medicines for cancer patients. *Evid Based Complement Alternat Med*. 2013; 2013: 3024-26.
9. Brami C, Bao T, and Deng G. Natural products and complementary therapies for chemotherapy-induced peripheral neuropathy: A systematic review. *Crit Rev Oncol Hematol*. 2016; 98: 325-34.
10. Hunter P. Alternative medicine on trial: clinical trials home in on complementary therapies and complex natural products. *EMBO Rep*. 2012; 13: 1062-5.
11. Yan H, and Jiang JG. Origin and concept of medicine food homology and its application in modern functional foods. *Food Funct*. 2013; 4: 1727-41.
12. Liu CX. Understanding "medicine and food homology", developing utilization in medicine functions. *Chinese Herbal Medicines*. 2018; 10: 337-8.
13. Liu L, Zhao YF, Han WH, et al. Protective effect of antioxidant on renal damage caused by doxorubicin chemotherapy in mice with hepatic cancer. *Asian Pac J Trop Med*. 2016; 9: 1101-4.
14. Selleri S, Seltmann H, Gariboldi S, et al. Doxorubicin-induced alopecia is associated with sebaceous gland degeneration. *J Invest Dermatol*. 2006; 126: 711-20.
15. Shih V, Wan HS, and Chan A. Clinical predictors of chemotherapy-induced nausea and vomiting in breast cancer patients receiving adjuvant doxorubicin and cyclophosphamide. *Ann Pharmacother*. 2009; 43: 444-52.
16. Liu H, Wang HY, Xiang DC, et al. Pharmaceutical measures to prevent doxorubicin-induced cardiotoxicity. *Mini Rev Med Chem*. 2017; 17: 44-50.
17. Guerreiro PS, Fernandes AS, Costa JG, et al. Differential effects of methoxyamine on doxorubicin cytotoxicity and genotoxicity in MDA-MB-231 human breast cancer cells. *Mutat Res*. 2013; 757: 140-7.
18. Thorn C, Oshiro C, Marsh S, et al. Doxorubicin pathways: pharmacodynamics and adverse effects. *Pharmacogenet Genomics*. 2011; 21: 440-6.
19. Bondza-Kibangou, Millot, Khoury E, et al. Antioxidants and doxorubicin supplementation to modulate CD14 expression and oxidative stress induced by vitamin D3 and seocalcitol in HL60 cells. *Oncol Rep*. 2007; 18: 1513-9.
20. Korac B and Buzadzic B. Doxorubicin toxicity to the skin: possibility of protection with antioxidants enriched yeast. *J Dermatol Sci*. 2001; 25: 45-52.
21. Baar MP, Brandt RMC, Putavet DA, et al. Targeted Apoptosis of Senescent Cells Restores Tissue Homeostasis in Response to Chemotoxicity and Aging. *Cell*. 2017; 169: 132-47 e16.
22. Cece R, Cazzaniga S, Morelli D, et al. Apoptosis of hair follicle cells during doxorubicin-induced alopecia in rats. *Lab Invest*. 1996; 75: 601-9.
23. Soni H, Pandya G, Patel P, et al. Beneficial effects of carbon monoxide-releasing molecule-2 (CORM-2) on acute doxorubicin cardiotoxicity in mice: role of oxidative stress and apoptosis. *Toxicol Appl Pharmacol*. 2011; 253: 70-80.
24. Chen T, Shen HM, Deng ZY, et al. A herbal formula, SYKT, reverses doxorubicin-induced myelosuppression and cardiotoxicity by inhibiting ROS-mediated apoptosis. *Mol Med Rep*. 2017; 15: 2057-66.
25. Nagai K, Oda A, and Konishi H. Theanine prevents doxorubicin-induced acute hepatotoxicity by reducing intrinsic apoptotic response. *Food Chem Toxicol*. 2015; 78: 147-52.
26. Elmore S. Apoptosis: a review of programmed cell death. *Toxicol Pathol*. 2007; 35: 495-516.
27. Oltvai ZN, Milliman CL, and Korsmeyer SJ. Bcl-2 heterodimerizes in vivo with a conserved homolog, Bax, that accelerates programmed cell death. *Cell*. 1993; 74: 609-19.
28. Zhu Y, Tchikonja T, Pirtskhalava T, et al. The Achilles' heel of senescent cells: from transcriptome to senolytic drugs. *Aging Cell*. 2015; 14: 644-58.
29. Francesco D' Agostini, Fiallo P, Ghio M, et al. Chemoprevention of doxorubicin-induced alopecia in mice by dietary administration of L-cystine and vitamin B6. *Arch Dermatol Res*. 2013; 305: 25-34.
30. Katoh M and Katoh M. Human FOX gene family (Review). *Int J Oncol*. 2004; 25: 1495-500.
31. Huang H and Tindall DJ. Dynamic FoxO transcription factors. *J Cell Sci*. 2007; 120: 2479-87.
32. Alexander SA. The contributions of nursing to genetics, epigenetics, genomics, and epigenomics: A word from the current president of ISONG. *Biol Res Nurs*. 2015; 17: 362-3.
33. Paus, R. Chemotherapy-induced alopecia in mice. Induction by cyclophosphamide, inhibition by cyclosporine A, and modulation by dexamethasone. *Am J Pathol*. 1994; 144: 719-34.
34. Allen RT, Hunter WJ, and Agrawal DK. Morphological and biochemical characterization and analysis of apoptosis. *J Pharmacol Toxicol Methods*. 1997; 37: 215-28.
35. Fukuda I, Tsutsui M, Yoshida T, et al. Oral toxicological studies of black soybean (Glycine max) hull extract: acute studies in rats and mice, and chronic studies in mice. *Food Chem Toxicol*. 2011; 49: 3272-8.
36. Hilmer SN. The hepatic pharmacokinetics of doxorubicin and liposomal doxorubicin. *Drug Metab Dispos*. 2004; 32: 794-9.
37. Su ZH, Ye J, Qin ZX, et al. Protective effects of madecassoside against Doxorubicin induced nephrotoxicity in vivo and in vitro. *Sci Rep*. 2015; 5: 18314.
38. Gross A, McDonnell JM, and Korsmeyer SJ. BCL-2 family members and the mitochondria in apoptosis. *Genes Dev*. 1999; 13: 1899-911.
39. Sharma S, Verma AK, Singh J, et al. Vitamin B6 tethered endosomal pH responsive lipid nanoparticles for triggered intracellular release of doxorubicin. *ACS Appl Mater Interfaces*. 2016; 8: 30407-21.
40. Kai C, Xiaolan Z, Heran D, et al. Clinical predictive models for chemotherapy-induced febrile neutropenia in breast cancer patients: a validation study. *PLoS One*. 2014; 9: e96413.
41. Laky B, Janda M, Kondalsamy-Chennakesavan S, et al. Pretreatment malnutrition and quality of life-association with prolonged length of hospital stay among patients with gynecological cancer: a cohort study. *BMC Cancer*. 2010; 10: 232.
42. Schaid DJ, Spraggs CF, McDonnell SK, et al. Prospective validation of HLA-DRB1*07:01 allele carriage as a predictive risk factor for lapatinib-induced liver injury. *J Clin Oncol*. 2014; 32: 2296-303.
43. Paus R, Haslam IS, Sharov AA, et al. Pathobiology of chemotherapy-induced hair loss. *Lancet Oncol*. 2013; 14: e50-9.
44. Lee EH, Cho SY, Kim SJ, et al. Overexpression of Bcl-2 protects from ultraviolet B-induced apoptosis but promotes hair follicle regression and chemotherapy-induced alopecia. *Am J Pathol*. 2000; 156: 1395-405.